

Preparation and characterization of ^{10}B targets at JRC-Geel

David Vanleeuw*, Jan Heyse, Goedele Sibbens, and Mariavittoria Zampella

European Commission, Joint Research Centre, Directorate G, Retieseweg 111, Geel B- 2440, Belgium

Abstract. Measurements of neutron-induced cross sections to generate nuclear data are a core activity of the JRC-Directorate G Standards for Nuclear Safety, Security and Safeguards unit in Geel. Thin ^{10}B layers are of great importance in this activity as they are used to measure the absolute neutron flux in the beam using the standard $^{10}\text{B}(n,\alpha)^7\text{Li}$ reaction cross-section as a reference. After a period of reduced activity and in line with a renewed interest for nuclear data, the demand for high quality ^{10}B targets increased. In this paper we describe the design and features of a new e-beam evaporator specifically customized for the preparation of boron targets as replacement of the old dysfunctional equipment. Several ^{10}B targets of varying thicknesses were prepared and characterized as part of the factory acceptance tests and implementation in the JRC-Geel target preparation laboratory. Differential substitution weighing was applied for mass determination and in order to calibrate the thickness monitor. Comparative time-of-flight measurements relative to ^{10}B and ^{235}U standard targets were conducted at the GELINA neutron time-of-flight facility at the JRC-Geel site as second methodology for the determination of ^{10}B areal density. The morphology of the layers was assessed by means of Scanning Electron Microscopy (SEM). The determination of impurities was realized by means of Energy Dispersive X-ray (EDX). Finally, two boron targets were prepared in the frame of the measurement of the neutron induced fission cross-section of ^{230}Th at the n_TOF neutron time-of-flight facility at CERN.

1 Introduction

The target preparation laboratory of the JRC in Geel was established in 1961. The first boron targets were prepared in 1967 by high frequency induction [1] and later on by e-beam evaporation for the preparation of boron reference standards for the neutron lifetime experiment [2]. By means of a Leybold Univex 450 e-beam evaporator, a set of ^{10}B reference targets was prepared and characterised by isotope dilution mass spectrometry and by irradiation in a thermal neutron beam. Despite the need of high quality and well characterised boron targets, the target preparation activities were stopped during the nineties due to a reorganisation of the JRC [3]. After the nuclear renaissance, the renewed interest for accurate nuclear data resulted in a new demand for high quality targets in order to provide the neutron facilities of the JRC in Geel with the necessary targets [4,5]. More specifically, high quality ^{10}B targets were requested for the absolute neutron flux monitoring of the beam by means of the $^{10}\text{B}(n,\alpha)^7\text{Li}$ reaction cross-section data as standard reference.

In view of this renewed interest, the target preparation activities were revived [6] and in a first stage the old Leighold Univex 450 e-beam evaporator was put back into service in 2009 after years of inactivity. Several boron targets were prepared with this equipment but poor signal after exposure to the neutron beam questioned the quality of the layers. The mass of the layers was therefore monitored at several time intervals

with a microbalance and by means of comparative weighing. This indicated a clear loss of mass in time which demonstrated the instability of the deposited layer, most likely due to the poor adsorption of the boron atoms as the original operational conditions could no longer be reached. This problem continued to persist despite the variation of parameters such as substrate type, deposition time and boron material. As neither the maximal power of the e-beam nor the vacuum in the chamber could be improved it was concluded that new equipment was required in order to comply with the demand for high quality boron targets. Efforts were made to acquire new highly enriched boron material but due to a lack of producers the boron stock of the target preparation laboratories was used.

In this paper we discuss the technical feasibility, acquisition and implementation of new deposition equipment for thin boron films. The technical features of the equipment are explained in relation with the specific needs for the preparation of boron targets and in view of emerging techniques in the field of thin layer deposition. The preparation of several boron targets of varying thicknesses is explained from factory acceptance tests (FAT) and start-up on up to the preparation of two large boron targets requested under a collaboration agreement with CERN in the frame of a neutron induced fission cross-section measurement of ^{230}Th at the n_TOF facility. Two techniques are applied for the determination of the boron and ^{10}B areal density of the layer and the calibration of the thickness monitor. The results of the Scanning Electron Microscope (SEM) and

* Corresponding author: david.vanleeuw@ec.europa.eu

Energy Dispersive X-ray (EDX) analysis for assessment of the layer quality and elemental composition are presented and discussed as well as further needs for characterisation.

2 E-beam evaporation

2.1 Deposition technique

Depending on whether the process is primarily chemical or physical, thin film deposition techniques fall into two broad categories, chemical vapor deposition or physical vapor deposition (PVD). Based on the acquired experience, the characteristics of boron and the requirements of the deposited layer in terms of purity and geometry, physical vapor deposition by thermal evaporation stood out as the most suitable technique. PVD processes are atomistic deposition processes in which material with high melting point and low vapor pressure is vaporized from a solid source in the form of atoms or molecules and transported in the form of a vapor through a vacuum or low pressure gaseous environment to the substrate, where it condenses. Thermal evaporation is a PVD process whereby the source material is thermally heated by means of resistance heating of a boat or by high energy electron beam (e-beam) heating of the source material itself and is used as a deposition technique for thin layers with a thickness in the range of a few nanometers to thousands of nanometers. The high melting point (2349 K) and heat of vaporization ($508 \text{ kJ}\cdot\text{mol}^{-1}$) of crystalline boron requires thermal evaporation by e-beam heating. When the high-speed electrons hit the boron in the water cooled crucible, sufficient energy is generated to melt and convert the boron material into vapor and then deposit it onto the substrate. The source to substrate distance can roughly be determined according to the required homogeneity (cosines law for a non-spherical surface) and yield (mean free path of molecules). In the case of higher flux processes such as electron-beam evaporation, collisions between evaporant atoms can lead to a focusing of the vapor plume [7]. Due to the low vapor pressure and hence low evaporation rate there are however no problems expected with the uniformity of the boron vapor.

2.2 Deposition equipment

The technical specifications for the e-beam evaporator were based on the experience with existing setups and on an evaluation of potentially interesting new features in order to gain more control over the deposition process. The distance to the single substrate stage was set at 40 cm (like in the previous setup), but it was extended with the possibility to move the substrate closer to the evaporation source for improved yield when thicker layers are requested (and decrease the deposition time as boron has a very low vapor pressure), or to increase the distance to guarantee homogeneity when larger samples are requested. The substrate stage can rotate with a speed

up to 40 rotations per minute and can hold a substrate with a maximum diameter of 12 cm. A stainless steel mask holding the substrate is mounted underneath the rotating stage and needs to be customized according to the requested spot size and the dimensions of the substrate. Frequently, very thin aluminised foils are requested as backings for the ^{10}B deposit in order to minimise energy loss of the emitted reaction particles in the backing. The fragility of these backings makes the cleaning prior to deposition difficult. In order to remove physically adsorbed hydrocarbon contamination from the surface of these backings which might interfere in the deposition process (adsorption of the boron atoms), it was decided to place a glow discharge module in front of the substrate stage. By means of ionized argon gas, the substrate can be cleaned prior to the deposition as the energetic plasma removes the weakly adsorbed contaminants [8,9]. Furthermore, the possibility to heat the substrate during and after deposition was added to the technical specifications in order to have control on the homologous temperature, which is the relation between the evaporation and sample temperature and is known to influence the morphology and quality of the layer according to the Structure-Zone Model of thin films [10].

After publication of the technical specifications and according to the European rules for public procurement, the contract for the development and construction of a new customized e-beam deposition system was awarded to Moorfield Nanotechnology®. The contract consisted of two phases where the construction phase was preceded by the conceptual phase (Fig. 1). In this phase, requiring approval prior to the construction phase, extensive collaboration based on the specific needs and practical experience with e-beam evaporation took place between the JRC Geel and Moorfield Nanotechnology®. The FAT consisted of the successful preparation of a boron target.

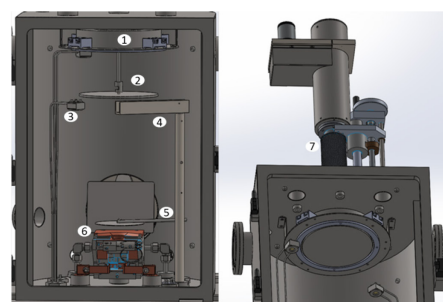


Fig. 1. 3D-design of the evaporation chamber: quartz heater (1), substrate holder (2), quartz crystal (3), glow discharge (4), shutter (5), evaporation source with e-beam (6), vertical movement substrate (7).

3 Preparation of boron targets

The final quality of the target depends on the quality of the starting material. This means that the material should be as pure as possible, highly enriched in the case of isotopes and preferably single element. For the implementation of the new evaporator we used

crystalline boron in the form of lumps with a chemical purity better than 98.0% as declared by the certificate of the provider. No specific enrichment was mentioned and the natural abundance of 19.9% of ^{10}B was assumed with a relative uncertainty of 3% [11]. Several boron targets were prepared as part of the acceptance tests, implementation, optimization and calibration of the equipment, characterization of the areal density and finally for a neutron time of flight experiment.

3.1 Targets for factory acceptance tests

Four test targets were prepared at the premises of Moorfield Nanotechnology® as part of the FAT and in order to establish the deposition parameters. The starting material was loaded in three of the six pockets protected with a tungsten liner in the copper crucible. The 0.5 mm thick aluminium substrates with a diameter of 50 mm were degreased with methanol and weighed by means of a Mettler-Toledo XP56 microbalance prior to deposition in view of applying differential weighing for the determination of the deposited mass. The height of the rotating substrate stage was set in the lowest position and a mask with a diameter of 30 mm was used to mount the substrate and define the spot size. All evaporations were conducted at a pressure better than 10^{-5} Pa which was a significant improvement compared to the old Leighbold evaporator (10^{-2} Pa). All features could be tested and approved (shutter, rotation of the pockets, rotation of the sample, vertical movement of the sample, heating of the sample). Each deposition run included prior in-situ cleaning with the argon plasma (10 minutes at gas flow of $30\text{ cm}^3\cdot\text{min}^{-1}$).

The optimal settings of the evaporation source were defined during the first evaporation runs by gradually increasing the power of the e-beam until a significant signal was registered by the thickness monitor (several $\text{\AA}\cdot\text{s}^{-1}$) and while applying high frequency sweeping. This occurred at the maximal current of 200 mA and resulted in a grey deposit, different from the expected appearance of a boron deposit as observed on reference boron targets prepared at JRC-Geel in the past. After further investigation, a small cavity could be observed in the tungsten liner indicating the evaporation of tungsten instead of only boron due to the high power of the e-beam. During the next two deposition runs, more attention was paid to the heat distribution of the e-beam by applying lower current (40 mA) and gently moving the e-beam instead of high frequency sweeping over a large area, resulting in a low deposition rate more in line with the low vapor pressure of boron. The two targets prepared under these conditions (FAT 3 and FAT 4) visually resembled the expected appearance of a boron deposit and were sent to JRC-Geel for mass determination and SEM/EDX analysis.

3.2 Targets for implementation and calibration

After confirmation of the quality of the last two FAT targets, the e-beam evaporator was installed in the JRC-Geel target preparation laboratory. In view of further

testing and implementation of the equipment as well as calibration of the thickness monitor, five more test deposits (Test 1 to 5) were prepared according to the previously defined deposition parameters on the same type of substrates and with the same spot diameter. In order to prepare deposits with increasing mass, five deposition runs ranging from 30 to 120 minutes were conducted at a pressure better than 5.10^{-5} Pa and an e-beam current between 30 and 40 mA. During the five deposition runs, the deposition rate ($\text{\AA}\cdot\text{s}^{-1}$) and final thickness (\AA) according to the thickness monitor were monitored. The settings of the thickness monitor were adapted according to the properties of boron as recommended by the Inficon manual (acoustic impedance of $22.699\text{ Pa}\cdot\text{s}\cdot\text{m}^{-1}$ and density of $2.370\text{ kg}\cdot\text{m}^{-3}$) and the unknown tooling factor was kept at 1 (see further). The final thickness of the layers was also determined by differential weighing of the masses of the deposited layers and by comparative neutron time-of-flight measurements at the GELINA facility.

3.3 Targets for cross section experiment

Finally, two targets were prepared in view of neutron induced-fission cross-section measurements at the neutron time-of-flight facility in CERN. The substrates consisted of 0.025 mm foils of aluminised Mylar with a diameter of 120 mm mounted on a aluminium ring with a thickness of 1 mm and inner diameter of 100 mm. These foils are too fragile to clean mechanically and only in-situ plasma cleaning was applied. The size of the substrate and the very low requested areal density of $8\text{ }\mu\text{g}\cdot\text{cm}^{-2}$ on an 80 mm spot size also excluded accurate differential weighing. The first target was therefore prepared according to the calibrated thickness monitor and measured by comparative time-of-flight measurement. The second target was prepared according to these results.

4 Characterization

4.1 Calibration thickness monitor

In order to deposit layers of a predefined thickness as defined by the target requestor, a reliable real time measurement during evaporation is required. The most common equipment for this purpose and also applied for the e-beam evaporator, is a quartz microbalance connected to a thickness monitor. A mass variation per unit area can be measured by the change in frequency of the water cooled quartz crystal resonator. As mass is deposited on the surface of the crystal, the thickness increases and consequently the frequency of oscillation decreases. This relationship was quantitatively established by Sauerbrey in 1959 [12] and further improved so that by introducing parameters inherent to the deposited material, such as density (the quartz crystal only measures the areal mass density) and acoustic impedance, the frequency change can be quantified and correlated precisely to the film thickness.

The thickness monitor measures however only the amount of material deposited on its sensor, not how much is deposited on the substrate. To avoid shadowing effects, the sensor cannot be placed in view of the substrate and may not even be at the same distance from it. Therefore, the rate at which the material is deposited on the sensor may not equal the rate at which it is deposited on the sample. The ratio of the two rates is called the "tooling factor (TF)" F_m and can be determined as follows:

$$F_m = F_i \cdot (T_m/T_i) \quad (1)$$

where F_i is the initial TF, T_i is the film thickness indicated by the instrument, and T_m is the actual, independently measured thickness of the deposited film. If no tooling factor has been pre-set or used before, F_i equals 1. Accurate weighing of the deposited layer with well-defined area is used as measurement method for the thickness of non-radioactive layers in the JRC-Geel target preparation laboratory [13] and was also applied for the boron targets. A second independent method was applied as confirmation.

4.2 Differential weighing

The methodology for thickness measurements of non-radioactive targets in the JRC-Geel laboratories consists of differential weighing of the target before and after deposition by means of substitution weighing according to the International Organization of Legal Metrology (OIML R111-1 : C.4 1-2) and defining the surface area of the deposit (spot) by applying a mask with well-known dimensions. Substitution weighing is a highly accurate and precise mass determination through comparison with mass standards to guarantee traceability to the SI units. Temperature, air pressure and humidity are measured for air buoyancy correction.

A Mettler-Toledo XP56 microbalance and a set of E2 calibration weights were used for all the weighing. Each target was weighed three times before and after deposition according to the SUUS method of substitution measurement where the Standard (S) and Unknown (U) are weighed in sequence after each other. The final masses were calculated after correction for air buoyancy and the combined standard uncertainties with a coverage factor $k = 1$ estimated in accordance with the Guide to the Expression of Uncertainty in Measurement [14]. The major uncertainty components result from the uncertainties on the mass standards, the balance parameters, the weighing and the diameter of the mask.

Obviously, the mass of the deposited layer takes all deposited elements into account, including other isotopes as well as the co-deposited impurities. If the impurities in the starting material are also deposited (which might happen due to the high evaporation temperature of boron, apart from the outgassing products before deposition which are retained by the shutter), the mass obtained by the differential weighing needs to be corrected for the purity of the boron and the enrichment in order to calculate the areal density of the ^{10}B .

Finally, differential weighing was also applied to verify the stability in time of the prepared boron targets.

4.3 Neutron time-of-flight measurement

A second independent characterization method for the amount of ^{10}B in the deposited film was applied. As previously mentioned, differential weighing takes all elements of the layer into account, so a method only measuring the amount of ^{10}B is more relevant. The second method consisted of mounting the prepared boron targets back-to-back with a fixed ^{10}B target on the cathode of a double, gas-filled, Frisch-gridded ionization chamber [15], and exposing them to one of the neutron beams of the GELINA neutron time-of-flight facility [16]. The fixed ^{10}B target is used as a neutron fluence monitor, in order to link consecutive measurements to each other.

As the $^{10}\text{B}(n,\alpha)^7\text{Li}$ reaction occurs, an α - and a ^7Li -particle are emitted in opposite directions. One of both charged particles will be emitted in the direction of the target backing, in which it will be stopped. The other particle will be emitted in the gas volume of the chamber, where it will ionize the gas due to interactions with the gas molecules. By applying an external voltage to the anode and cathode, the electrons and positive ions resulting from the ionization will start moving in opposite directions and induce a charge on both electrodes. When the electrodes are connected to an external read-out system, the induced charge will produce an electronic signal which can be registered. The amplitude of the signal will be proportional to the energy of the ionizing particle (i.e. α or ^7Li).

The reaction cross section, which is a measure for the reaction probability, is well-known for the $^{10}\text{B}(n,\alpha)^7\text{Li}$ reaction and considered a standard in the neutron energy range between thermal neutron energy and 1 MeV [17]. As such, the number of reactions registered by either side of the ionization chamber, allows determining the neutron fluence as a function of neutron energy if the areal density of ^{10}B nuclei in the boron target is well-known; or, alternatively, it allows determining the number of ^{10}B nuclei in a ^{10}B target if the neutron fluence as a function of neutron energy is well-known.

Two ^{10}B reference samples with different areal density were used for calibrating the ionization chamber. These samples were characterised by neutron activation in the BR2 research reactor of the SCK-CEN with a well-known neutron fluence in the frame of the accurate measurement of the neutron lifetime [2]. By consecutively putting both reference samples in the ionization chamber, back-to-back with the fixed ^{10}B monitor sample, it was possible to deduce and verify a correlation between the neutron fluence at the position of the reference sample and the response of the detector on the side with the fixed ^{10}B sample.

An additional verification was done by placing a well-known ^{235}U sample in the same position as the reference samples and by using the standard reaction cross section for the $^{235}\text{U}(n,f)$ reaction at thermal neutron energy [17].

The samples produced with the new e-beam evaporator were consecutively mounted in the position of the reference samples. Their areal density for ^{10}B nuclei was determined, using the known neutron fluence deduced from the response of the fixed ^{10}B sample side of the chamber and the standard cross section for the $^{10}\text{B}(n,\alpha)^7\text{Li}$ reaction.

4.4 SEM-EDX

The morphology of the layer of several boron targets was investigated by means of a JSM-7800F Schottky Field Emission Scanning Electron Microscope (SEM) in high vacuum mode. Images were taken in low depth focus at 10X magnification for the general appearance of the sample and in SEM mode at magnifications of 250X and 1000X on several positions. For all the image acquisitions the accelerating voltage was 20 kV and the lower secondary electron detector was used.

An elemental analysis was performed by Energy Dispersive X-ray spectroscopy (EDX) to confirm the

presence of boron and check the presence of impurities and more specifically the absence of tungsten from the liner of the crucible. This was done in the center of the sample at a working distance of 10 mm and at different penetration depths by varying the accelerating voltage from 1 to 30 kV. The acquisition time was 60 s and the spectra were normalized. The results are qualitative and the reported weight percentage values are indicative only.

5 Results and discussion

After determination of the appropriate settings of the e-beam (power and sweeping), nine boron targets were prepared (Table 1): two targets for the FAT (FAT3 and FAT4), five targets for the calibration and implementation in the target preparation laboratories (test 1 to 5) and finally two targets in view of a neutron time-of-flight experiment at CERN (TP2017-10-01 and 02).

Table 1 Overview of the boron deposits prepared with the new e-beam evaporator

Target	e-beam current (mA)	Deposited mass (g)	Areal Density, weighing ($\mu\text{g}/\text{cm}^2$)	Areal Density B10, weighing and natural abundance ($\mu\text{g}/\text{cm}^2$)	Areal Density B10, TOF ($\mu\text{g}/\text{cm}^2$)	SEM	EDX
FAT 1 and 2	200	-	-	-	-	-	-
FAT 3	30 -40	0.000142(14)	20.2(8)	4.0(2)		Some dust particles, layer follows Al morphology	B, Al, O, Fe traces, no W
FAT 4	30-40	0.000260(13)	36.8(24)	7.3(5)		Some dust particles, layer follows Al morphology	B, Al, O, Fe traces, no W
Test 5	30-40	0.000039(18)	5.6(25)	1.1(5)			
Test 4	30-40	0.000079(17)	11.1(25)	2.2(5)			
Test 3	30-40	0.000154(18)	21.8(26)	4.3(5)			
Test 2	30-40	0.000289(18)	40.8(30)	8.1(6)	7.0		
Test 1	30-40	0.000527(19)	74.5(40)	14.8(9)	12.7	Some dust particles, layer follows Al morphology	B, Al, O, Fe traces, no W
TP2017-10-01	30-35	no weighing	8.0 according monitor	2.8 calculated according monitor	2.9		
TP2017-10-02	30-35	no weighing	22.2 according monitor	8.0 calculated according monitor			

Visually, all deposits show a good layer quality and different colors are observed at different layer thicknesses due to a varying reflection of visible light (Fig. 2). Despite some dust particles, the layer is smooth and follows the roughness profile of the unpolished aluminum substrates as can be seen on the SEM images (Fig. 3). This proves the good adhesion of the boron layer which is also confirmed by the layer stability, verified by regular weighing. The layers deposited with the new e-beam evaporator are thus clearly of much better quality than those prepared with the old Leybold evaporator.



Fig. 2. Pictures five boron test targets prepared at JRC-Geel

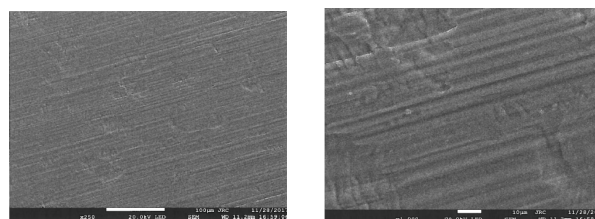


Fig. 3. SEM image of FAT 3 at magnification 250X (left) and 1000X (right) with same centre point

The EDX analysis at different penetration depths (1 kV, 5 kV and 30 kV) confirms the presence of boron and the absence of tungsten from the liner placed in the crucible. The thickness of the boron layer is smaller than the average penetration depth at 30 kV as demonstrated by the increase of the boron mass fraction at decreasing acceleration voltages. Aluminum and oxygen were also detected and are most probably present in the form of aluminum oxide in the top layer of the substrate. Metallic aluminum is very reactive with atmospheric oxygen and a 4 nm aluminum oxide layer forms on any exposed aluminum surface [18]. Traces of iron (0.1 wt%) were detected at 30 kV with 10 min

acquisition time. The EDX results indicate that the deposited layer is not affected by impurities coming from the starting material; this may depend on the high purity of the starting material and/or on the absence of co-evaporation.

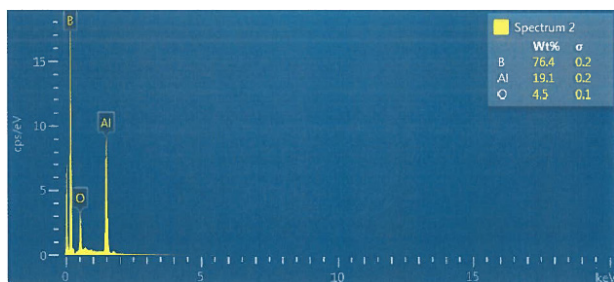


Fig. 4. EDX spectrum of Test 1 taken at the centre of the sample at 5 kV

Table 2 Calculation of the Tooling Factor

B Target	Measured thickness monitor (Å)	Measured total mass layer (g)	Calculated areal density ($\mu\text{g}/\text{cm}^2$)	Calculated thickness (nm)	Calculated Tooling Factor
test 5	125	0.000039(18)	5.6(25)	24(11)	188(85)%
test 4	250	0.000079(17)	11.1(25)	47(10)	188(43)%
test 3	500	0.000154(18)	21.8(26)	92(10)	184(24)%
test 2	760	0.000289(18)	40.8(30)	172(11)	227(20)%
test 1	1500	0.000527(19)	74.5(40)	314(11)	210(15)%

The thickness of the boron layers deposited on the aluminum substrates as determined by differential weighing for a spot size with a diameter of 30 mm as defined by the mask corresponds to an areal density varying from 5.6 to 74.5 $\mu\text{g}\cdot\text{cm}^{-2}$. For the five test targets, these results were compared with the readouts of the thickness monitor (Fig. 5) and show a significant linear correlation ($p < 0.05$, $r = 0.997$), meaning that within an uncertainty range the thickness monitor can be used to deposit a predefined thickness. Besides for the direct preparation of a specific layer thickness, this is of particular importance for very thin layers on large substrates unsuitable for thickness determination by weighing.

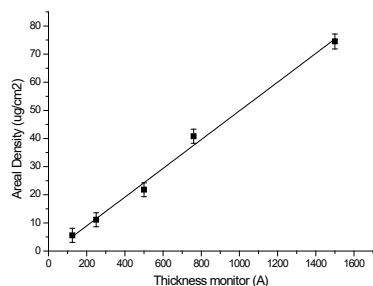


Fig. 5. Graphic representation of the readout of the thickness monitor and the areal density according to weighing

After conversion of the areal density to the thickness of the boron layer by means of the density of metallic boron, the TF for each deposit was calculated according to equation 1 (Table 2). We notice an important fluctuation of the TF which in this case can be explained

by the large uncertainty on the weighing results of the thin boron layers used to calculate the layer thickness. As by experience the TF appears to be more stable when evaporating powder by resistance heating and when taking a closer look at the boron material during and after evaporation, this fluctuation might also find its origin in shadowing effects or the non-uniform evaporation. Due to the properties of metallic boron, the evaporation takes place more locally where the e-beam hits and heats up the crystalline boron lump. This creates moving craters in the material and continuously modifies the geometry and hence TF, which should be a fixed value with fixed geometry of the sample size and height, evaporation source and crystal.

As no impurities are detected by EDX (above the detection limits and except for 0.1 wt% Fe) and no enriched boron was used, the areal density of ^{10}B can directly be calculated with the natural abundance of ^{10}B (Table 1). A second method was applied for direct determination of this value by comparing the response of a double Frisch-gridded ionization chamber for the test targets 1 and 2 with the response of two reference boron targets with well-known areal density of ^{10}B (originating from the neutron lifetime project [2]) and a ^{235}U sample with a well-known areal density. Both targets were mounted consecutively in the ionization chamber, back-to-back with a fixed ^{10}B sample used as neutron fluence monitor, and put in one of the neutron beams of the GELINA neutron time-of-flight facility. Preliminary results of these measurements, point to an amount of ^{10}B which is 15% lower than expected. An in-depth analysis of the results obtained with the time-of-flight technique, including an uncertainty analysis, is ongoing. With an uncertainty on the weighing of 3 to 6%, the preliminary results might point to an overestimation of the amount of ^{10}B based on the weighing and natural enrichment. This might be due to the presence of undetected impurities in the boron layer (below the detection limit of EDX) or more probably due to a lower enrichment of the starting material. In order to clarify the reason of this discrepancy, also in view of the use of other batches of enriched boron, it is therefore necessary to assess the purity and the isotopic composition of the different boron starting materials stored for a long time in the target preparation laboratory. This will be done at JRC-Karlsruhe by combining different techniques based on mass spectrometry. The total content of boron in the starting materials will be measured by isotope dilution mass spectrometry (IDMS) with an inductively coupled plasma mass spectrometry (ICP-MS) instrument. IDMS is considered the most precise method for quantitative determinations of the concentration of multi-isotopic elements and ICP-MS is the most used technique for boron determinations among present-day technologies [19]. Due to its low detection limits (at ppb level) ICP-MS will also be used to check the eventual presence of impurities in the boron starting materials by multi-element analysis. The isotopic composition of the boron starting materials will be measured by thermal ionization mass spectrometry (TIMS) which is a technique that can provide a high degree of accuracy and precision of the measurement results [20].

In order to prepare the large ^{10}B deposits with a thickness of $8\ \mu\text{g}\cdot\text{cm}^{-2}$ as requested by CERN, the real time measurement of the thickness monitor according to the previously determined tooling factor of 210% for test 1 was applied for target TP2017-10-01. Due to the large uncertainty on the TF and as the areal density could not be determined by differential weighing, the target was measured relative to the boron standards, resulting in a much lower thickness than expected (Table 1). Closer examination of the positioning of the much larger substrate stage in the evaporation chamber showed a shadowing effect of the quartz crystal resulting in a larger TF than previously calculated. Based on the last results, a new correction factor was applied for the preparation of the second target TP2017-10-02. The latter could not be characterized due to the planning of neutron induced fission cross-section measurement of ^{230}Th .

6 Conclusion

A new e-beam evaporation system customized according to the specific needs for the deposition of thin boron layers and based on the latest available thin layer technology was acquisitioned following the public procurement rules and successfully implemented by conducting several evaporation runs. The prepared boron targets visually resemble the reference boron targets and further assessment by SEM-EDX analysis confirms a smooth and well adsorbed layer without defects or impurities originating from the starting material or evaporation liner. Accurate differential weighing was applied to determine the total areal density and monitor the stability of the layers. Five test deposits of different thicknesses were prepared to calibrate the thickness monitor. The areal density of ^{10}B was determined by comparing these targets with ^{10}B and ^{235}U reference deposits in a double Frisch-gridded ionization chamber and exposing them to one of the neutron beams of the GELINA facility. The results are in line with the expected natural enrichment but the deviation between both characterization methods requires the need of further and more accurate characterization of the starting material. Finally, the acquired experience in terms of preparation and characterization was applied to provide two thin boron targets for CERN in view of a neutron time-of-flight experiment.

After a decade of technical incapability, the target preparation laboratory is once again able to prepare high quality boron targets which are of great importance for the determination of the neutron flux in the frame of nuclear data research.

References

1. J. Van Audenhoven, J. Joyeux, Nucl Inst and Methods **57**, 157 (1967)
2. J. Pauwels, R. Eyckens, A. Lamberty, J. Van Gestel and H. Tagziria, R.D. Scott, J. Byrne, P.G. Dawber,

- D.M Gilliam, Nucl. Instrum. Methods Phys. Res. A **303**, 133-140 (1991)
3. J. Van Audenhove, J. Pauwels, J. Jaklovsky (Eds.), *Preparation of Nuclear Targets for Particle Accelerators*, 79-87 (1981)
4. <https://ec.europa.eu/jrc/en/research-topic/neutron-data> Accessed on 02/08/2018
5. A. Plompen, JRC-IRMM, AIP Conf. Proc. **769**, 1417 (2005)
6. A. Stolarz, R. Eykens, A. Moens, Y. Aregbe, Nucl. Instrum. Methods Phys. Res. A **613**, 351–356 (2010)
7. A. Powell, P. Minson, G. Trapaga, U. Pal, Metall. Trans. A **32**, 8, 1959-1966 (2001)
8. Staff of Kaufman & Robinson Inc, Technical Note KRI-06
9. A. Belkind, S. Gershman, *Vacuum Technology & Coating* (2008)
10. J.A. Thornton, Proc. SPIE **0821**, Modeling of Optical Thin Films, 95-103 (1988)
11. S. Szegedi, M. Váradi, C. Buczkó, M. Várnagy, T. Sztaricskai, J. Radioanal Nucl. Chem. **146** (3), 177 (1990)
12. G.Z. Sauerbrey, Phys, **155**, 206–222 (1959)
13. D. Sapundjiev, A. Dean, U. Jacobsson, K. Luyckx, A. Moens, G. Sibbens, R. Eykens, Y. Aregbe, Nucl. Instrum. Methods Phys. Res. A **686**, 75–81 (2012)
14. <https://www.bipm.org/en/publications/guides/gum.html>
15. C. Budtz-Jørgensen, H.-H. Knitter, Ch. Straede, F.-J. Hamsch, R. Vogt, Nucl. Instrum. Methods Phys. Res. A **258**, 209-220 (1987)
16. W. Mondelaers, P. Schillebeeckx, Notiziario Neutroni e Luce di Sincrotrone **11** (2), 19-25 (2006)
17. A.D. Carlson, V. G. Pronyaev, R. Capote, G. M. Hale, Z.-P. Chen, I. Duran, F.-J. Hamsch, S. Kunieda, W. Mannhart, B. Marcinkevicius, R. O. Nelson, D. Neudecker, G. Noguere, M. Paris, S. P. Simakov, P. Schillebeeckx, D. L. Smith, X. Tao, A. Trkov, A. Wallner, W. Wang, Nuclear Data Sheets **148**, (143-188)2018)
18. T. Campbell, R. Kalia, A. Nakano, P. Vashishta, S. Ogata, S. Rodgers, Phys. Rev. Lett. **82** (24), 4866 (1999)
19. R.N. Sah, P.H. Brown, Microchem. J., **56**, 285-304 (1997)
20. R.N Sah, P.H Brown, Biological Trace Element Research **66**, 39-53 (1998)